

# Imaging with Diffractive Axicons rapidly milled on Sapphire by Femtosecond Laser Ablation

Daniel Smith <sup>1\*</sup>, Soon Hock Ng <sup>1</sup>, Molong Han <sup>1</sup>, Tomas Katkus <sup>1</sup>, Vijayakumar Anand <sup>2\*</sup>, and Saulius Juodkazis <sup>1,3</sup>

<sup>1</sup> Optical Sciences Centre and ARC Training Centre in Surface Engineering for Advanced Materials (SEAM), School of Science, Computing and Engineering Technologies, Swinburne University of Technology, Hawthorn, VIC 3122, Australia; danielsmith@swin.edu.au (D.S.); vanand@swin.edu.au (V.A.); tkatkus@swin.edu.au (T.K.)

<sup>2</sup> Institute of Physics, University of Tartu, Ülikooli 18, 50090 Tartu, Estonia

<sup>3</sup> World Research Hub Initiative (WRHI), School of Materials and Chemical Technology, Tokyo Institute of Technology, 2-12-1, Ookayama, Meguro-ku, Tokyo 152-8550, Japan

\* Correspondence: danielsmith@swin.edu.au (D.S.); vanand@swin.edu.au (V.A.)

**Abstract:** We show that a single pulse burst fabrication will produce a flatter and smoother profile of axicons milled on sapphire compared to a pulse overlapped fabrication which will result in a damaged and a much rougher surface. The fabrication of large area (sub-1 cm cross-section) micro-optical components in a short period of time (~ 10 min) and with lesser number of processing steps is highly desirable and cost-effective. Our results were achieved with femtosecond laser fabrication technology which has revolutionized the field of advanced manufacturing. This study compares three configurations of axicon such as the conventional axicon, a photon sieve axicon (PSA) and a sparse PSA directly milled onto a sapphire substrate. Debris of redeposited amorphous sapphire was removed using isopropyl alcohol and potassium hydroxide. A spatially incoherent illumination was used to test the components for imaging applications. Non-linear reconstruction was used for cleaning noisy images generated by the axicons.

**Keywords:** ablation; femtosecond lasers; diffractive optical elements; imaging; astronomy



check for  
updates

**Citation:** Smith, D. et al. Imaging with Diffractive Axicons on Sapphire. *Eng. Proc.* **2022**, *1*, 0. <https://doi.org/>

**Academic Editor:** Firstname  
Lastname

Published:

**Publisher's Note:** MDPI stays neutral with regard to jurisdictional claims in published maps and institutional affiliations.



**Copyright:** © 2022 by the authors. Licensee MDPI, Basel, Switzerland. This article is an open access article distributed under the terms and conditions of the Creative Commons Attribution (CC BY) license (<https://creativecommons.org/licenses/by/4.0/>).

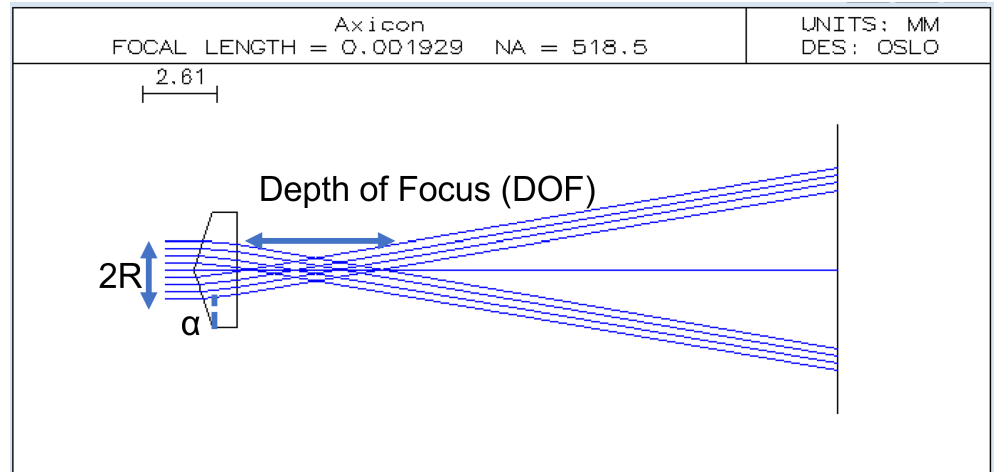
## 1. Introduction: Axicons and Photon Sieves

Axicons are diffractive optical elements which have a line focus. Importantly axicons are Bessel beam generators and can be used for a range of different applications including optical trapping [1,2]. Bessel beams are important as they are diffraction resistant and can be used for optical imaging applications [3] and biomedical applications like ultrasound imaging [4–6].

In this body of work, it is described an optimal and record time processing of micro-optical components where the processes used is much shorter and more cost effective than previous attempts. Instead of using axicon lenses, micro-optical binary, surface axicons with two phase or amplitude configurations are used. The extra configurations gave rise to, in total, three different diffractive optical elements, a conventional surface axicon, surface photon sieve axicon (PSA), and sparse surface photon sieve axicon (sparse PSA) which were directly milled onto a sapphire substrate.

This particular micro-optical component falls in the category of diffractive optics and plays an important role in many areas of research and have been manufactured with different techniques. The techniques generally employed are photolithography [7], electron beam lithography [8], and ion beam lithography [9], which are time consuming and expensive making the device itself expensive. Femtosecond laser ablation is superior to all of the above methods with only one exception the ability to deliver a practical solution for large area such as mm-to-cm scale micro-optical element fabrication [10–13].

Lately there has been a shift in focus in imaging research from using coherent light sources to incoherent ones due to the many advantages such as broad applicability, low



$$DOF = \frac{R\sqrt{1-n^2 \sin^2(\alpha)}}{\sin^2(\alpha) \cos^2(\alpha) (n \cos(\alpha) - \sqrt{1-n^2 \sin^2(\alpha)})} \approx \frac{R}{(n-1)\alpha}$$

**Figure 1.** Conventional axicon lens simulated in OSLO software for application at wavelength of 550 nm. Depth of field equation for conventional axicon lens.

cost, and high resolving power. We have used femtosecond fabrication by ablation to rapidly fabricate two-level axicons directly on to sapphire substrates. Two configurations, conventional ring - and sieve configurations were produced. Furthermore, our work focused on the rapid fabrication to manufacture large area diffractive optical elements for astronomical imaging applications.

The beam characteristics were investigated for a spatially incoherent illumination since it is available at low cost and is therefore relevant to large scale astronomical applications. In astronomy, large area devices are required which can be easily manufactured using femtosecond fabrication systems. The optical configuration of light diffracted from a point object is incident on a diffractive axicon and the intensity distribution is recorded (shown in figure 2).

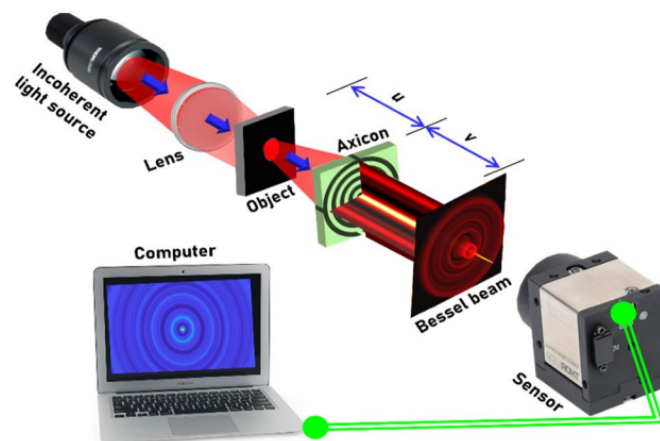


**Figure 2.** Optical configuration for the generation of Bessel beams by a diffractive axicon.

## 2. Results and Discussion: Laser Ablation and Imaging

The fabrication was carried out on a sapphire substrate 500 μm in thickness and 10 mm by 10 mm in size. Sapphire has a refractive index of  $n_{sapphire} = 1.76$  and has a spectral window from 300 nm to 6000 nm. The milling depth,  $t$ , is determined by the relationship between the wavelength that the diffractive optical element is desired to interact with and

the refractive index of the material ( $t = \lambda/2(n_{\text{sapphire}} - 1)$ ). The thickness  $t$  was determined to be  $400\mu\text{m}$  for  $\lambda \approx 600\text{ nm}$ .  $617\text{ nm}$  is the wavelength source for optical testing. Acetone and Iso-Propyl Alcohol were used to clean the substrate prior to fabrication.

Three optical devices; a conventional surface axicon, surface photon sieve axicon (PSA), and sparse surface photon sieve axicon (sparse PSA) were created using light conversion's PHAROS laser operating at  $200\text{ kHz}$  repetition rate,  $\lambda = 1030\text{ nm}$  wavelength,  $2.5\text{ W}$  average power,  $230\text{ fs}$  pulse duration and a  $5\times$  magnification,  $NA = 0.14$  numerical aperture Mitutoyo Plan APO NIR infinity corrected objective lens.

Two pulses per ablation spot was used to ablate the regions of the axicon as a consequence these more heavily overlapped regions incurred ripple formation. The attenuator serves to create more precise beam energies in combination with the objective lens. Here a  $5\mu\text{J}$  beam was used to achieve the fabrication which lead to pulse energies on the order of  $70\text{ TW}/\text{cm}^2$  even when the ablation threshold of sapphire is only on the order of  $10\text{ TW}/\text{cm}^2$  and ablation spots with diameter of  $8.9\mu\text{m}$ .

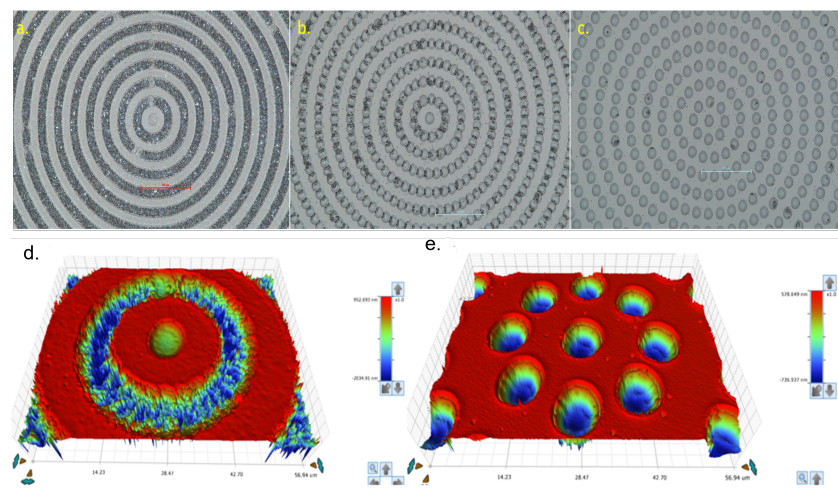


**Figure 3.** Optical microscope images of the three different devices created: a conventional surface axicon (a), surface photon sieve axicon (PSA) (b), and sparse surface photon sieve axicon (sparse PSA) (c). Below, the optical profilometer images of the conventional surface axicon (d) and and sparse surface photon sieve axicon (sparse PSA) (e)

The optical testing was carried out using a high-power LED and a spectral filter to improve the temporal coherence. A pinhole with a size of  $100\mu\text{m}$  and a cross shaped object were used for imaging. A  $3\times$  magnifying system was used to re-image the intensity distribution that is close to the diffractive optical elements on an image sensor. These optical elements were mounted one after the other and the intensity distributions were recorded at  $5\text{ mm}$  for the axicon, PSA and sparse PSA. The pinhole was replaced by a cross object and the intensity patterns again were recorded at  $3\text{ cm}$  from the DOEs. Again, the images were cleaned using non-linear reconstruction and to further improve the cleaning results, additional filters such as a median filter and correlation filters were used. Significant difference was seen in the cleaned images compared to the original images without filters.

### 3. Conclusions and Future Works

This study showed that the fabrication time could be cut to  $10\text{ min}$  using the femtosecond laser fabrication method for large area of  $5\text{ mm} \times 5\text{ mm}$  objects. It was noticed that when the beam overlap during milling resulted in redeposition of material resulting in a lower depth than the case without beam overlap which goes against the common belief that overall higher exposure with the beam overlap increases the depth. An increase in roughness has been noticed and it is contributed by the redeposition and to light-matter interaction at temperature changes due to the ablation process. It is noted that debris will have to be reduced to avoid a build-up of rough areas. Some of the latest developments in

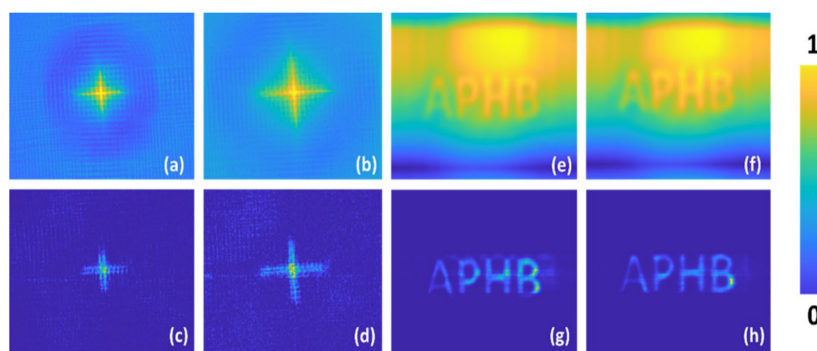


**Figure 4.** Intensity distribution of cross object recorded at (a)  $z=5$  cm and (b)  $z=6$  cm and the corresponding cleaned images (c)  $z=5$  cm and (d)  $z=6$  cm, respectively. Intensity distribution of synthetic object ‘APHB’ recorded at (e)  $z=5$  cm and (f)  $z=6$  cm and the corresponding cleaned images (g)  $z=5$  cm and (h)  $z=6$  cm, respectively.

astronomical spectral imaging technologies such as FOBOS require numerous micro-optical devices for the successful implementation of free space to fiber bundle coupling for spectral imaging. The current work shows the possibility of rapid fabrication and beam cleaning capable of supporting retrieving spatial information in addition to the recorded spectral information.

**Author Contributions:** Conceptualisation, S.J., V.A., S.H.N.; investigation, D.S., V.A., T.K.; writing—original draft preparation, D.S.; review and editing, all authors. All authors have read and agreed to the published version of the manuscript.

**Funding:** This research was funded by the Australian Research Council, grant number LP190100505. S.J. is grateful for startup funding from the Nanotechnology Facility at Swinburne and to the Workshop-on-Photonics for the technology transfer project, which installed the first industrial-grade microfabrication setup in Australia. Part of this study was made during a Grand Challenge undergraduate project of A.T.

**Institutional Review Board Statement:** Not applicable

**Informed Consent Statement:** Not applicable

**Data Availability Statement:** The data presented in this study are available on request from the corresponding author.

**Conflicts of Interest:** The authors declare no conflicts of interest.

## References

1. Ding, Z.; Lai, G. Enhancement of axial optical trapping force using a pair of axicons. Technical Digest. CLEO/Pacific Rim '99. Pacific Rim Conference on Lasers and Electro-Optics (Cat. No.99TH8464), 1999, Vol. 2, pp. 369–370 vol.2. doi:10.1109/CLEOPR.1999.811474.
2. Balasubramani, V.; Vijayakumar, A.; Rai, M.R.; Rosen, J.; Cheng, C.J.; Minin, O.V.; Minin, I.V. Binary square axicon with chiral focusing properties for optical trapping. *Optical Engineering* **2019**, *59*, 1. doi:10.1117/1.oe.59.4.041204.
3. Khonina, S.N.; Kazanskiy, N.L.; Karpeev, S.V.; Butt, M.A. Bessel Beam: Significance and Applications—A Progressive Review. *Micromachines* **2020**, *11*. doi:10.3390/mi11110997.
4. Hsu, D.K.; Margetan, F.J.; Thompson, D.O. Bessel beam ultrasonic transducer: Fabrication method and experimental results. *Applied Physics Letters* **1989**, *55*, 2066–2068, [<https://doi.org/10.1063/1.102107>]. doi:10.1063/1.102107.
5. Yu Lu, J.; Song, T.; Kinnick, R.; Greenleaf, J. In vitro and in vivo real-time imaging with ultrasonic limited diffraction beams. *IEEE Transactions on Medical Imaging* **1993**, *12*, 819–829. doi:10.1109/42.251134.
6. Lu, J.Y.; Xu, X.L.; Zou, H.; Greenleaf, J. Application of Bessel beam for Doppler velocity estimation. *IEEE Transactions on Ultrasonics, Ferroelectrics, and Frequency Control* **1995**, *42*, 649–662. doi:10.1109/58.393108.

7. Kondo, T.; Juodkazis, S.; Mizeikis, V.; Misawa, H.; Matsuo, S. Holographic lithography of periodic two- and three-dimensional microstructures in photoresist SU-8. *Opt. Express* **2006**, *14*, 7943–7953. doi:10.1364/OE.14.007943.
8. Anand, V.; Ng, S.H.; Katkus, T.; Juodkazis, S. White light three-dimensional imaging using a quasi-random lens. *Opt. Express* **2021**, *29*, 15551–15563. doi:10.1364/OE.426021.
9. Seniutinas, G.; Gervinskas, G.; Anguita, J.; Hakobyan, D.; Brasselet, E.; Juodkazis, S. Nanoproximity direct ion beam writing. *Nanofabrication* **2016**, *2*. doi:10.1515/nanofab-2015-0006.
10. Marcinkevičius, A.; Juodkazis, S.; Watanabe, M.; Miwa, M.; Matsuo, S.; Misawa, H.; Nishii, J. Femtosecond laser-assisted three-dimensional microfabrication in silica. *Opt. Lett.* **2001**, *26*, 277–279. doi:10.1364/OL.26.000277.
11. Malinauskas, M.; Žukauskas, A.; Hasegawa, S.; Hayasaki, Y.; Mizeikis, V.; Buividas, R.; Juodkazis, S. Ultrafast laser processing of materials: from science to industry. *Light: Science & Applications* **2016**, *5*, 2047–7538. doi:10.1038/lssa.2016.133.
12. Juodkazis, S.; Yamasaki, K.; Mizeikis, V.; Matsuo, S.; Misawa, H. Formation of embedded patterns in glasses using femtosecond irradiation. *Applied Physics A* **2004**, *4*, 1549–1553. doi:10.1007/s00339-004-2845-1.
13. Vanagas, E.; Kudryashov, I.; Tuzhilin, D.; Juodkazis, S.; Matsuo, S.; Misawa, H. Surface nanostructuring of borosilicate glass by femtosecond nJ energy pulses. *Applied Physics Letters* **2003**, *82*, 2901–2903, [<https://doi.org/10.1063/1.1570514>]. doi:10.1063/1.1570514.